Bound States in Photonic Fabry–Perot Resonator Comprised of Two Nonlinear Off-Channel Defects[¶]

E. N. Bulgakov[a, b] and A. F. Sadreev[a]

[a] *Institute of Physics, Academy of Sciences, Krasnoyarsk, 660036 Russia*
[b] *Siberian State Aerospace University, Krasnoyarsk, Russia*

Two off-channel nonlinear defects coupled to the photonic waveguide constitute the Fabry–Perot interferometer (FPR). The defects are made from a Kerr-like nonlinear material. For the linear case such a FPR can support the bound states in the form of standing waves between the defects if the distance between them is quantized. For the nonlinear case the bound states appear for arbitrary distance between the defects however for an quantized electromagnetic intensity. For the transmission through FPR we reveal new resonances and show these are a result of coupling of the bound states with incident wave because of nonlinearity of the defects. The resonances are spaced at the eigen frequencies of bound states.

1. INTRODUCTION

The Fabry-Perot resonator (FPR) consists of two plane mirrors at the distance L and dielectric media with the refractive index n between as shown in Fig. 1a. Then the transmission through the FPR can be easily found as geometric sum of consequent transmissions and reflections through each mirror specified by t_1 and r_1 respectively

$$t = \frac{t_1^2 \exp(ikL)}{1 - r_1^2 \exp(2ikL)}, \qquad (1)$$

where $k = \omega n/c$ is the wave number in a media with the refraction index n between mirrors. For metallic perfect mirrors in optical region of frequencies one can disregard the dependence of the reflection $r_1 = 1$ on the frequency to obtain that the bound state which does not leaks through the mirrors arises at $kL = \pi m$. We refer the reader to [1] for more details of this phenomenon in the FPR. Therefore, the underlying mechanism of the bound states in the FPR is (i) perfect reflections at mirrors and (ii) the integer number of the half waves are to be spaced between mirrors.

This FPR approach, exclusively transparent, was applied to photonic crystal (PC) structure with one and two waveguides coupled with two off-channel single-mode cavities [2–7] (see Figs. 1b, 1c), to typical one-dimensional double-barrier structure with temporally periodically driven potential of barrier [8] and two identical quantum dots connected by wire [9–11]. The bound states whose frequencies are in a propagation band of the waveguide can be classified as the

bound states in continuum (BSC) [12, 13]. There are also bound states of the defects with eigen frequency ω_0. However because of coupling of the defects with the waveguide they become extended. While the BSC has no coupling with continuum (waveguide) [14, 15] and therefore can not be excited by transmitted wave [16] in linear systems. It can be traced by narrowing of the resonance width for approaching to the BSC point [17–19].

The reader is reminded that a photonic crystal is a periodic array of dielectric media [20] having electro-
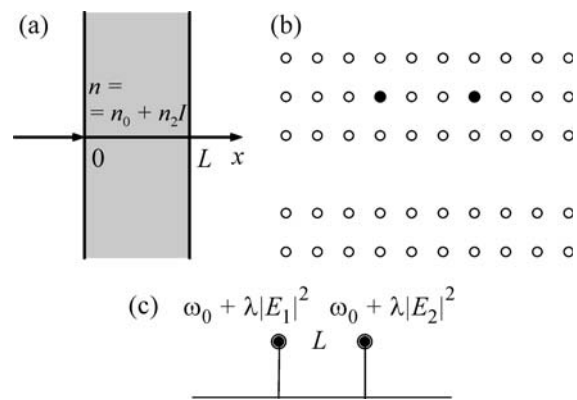
Fig. 1. (a) A view of transmission through the Fabry–Perot resonator filled by nonlinear media [1]. (b) Photonic crystal consists of a square lattice of dielectric rods. A single row of rods is extracted to form one-dimensional directed waveguide. Two nonlinear defect rods marked by filled circles are inserted near the waveguide. (c) The model Fan et al. [3] which describes the real PC structure shown in (b).

[¶]The article is published in the original.

magnetic modes that are Bloch waves with a frequency spectrum separated into a series of pass and stop bands. We consider a square array of parallel, infinitely long high dielectric rods in air. The removal of a row of rods breaks the periodicity in one spatial direction. If the parameters of the crystal are such that there is a complete band gap for wave vectors perpendicular to the rods, then this defect can introduce modes that decay exponentially away from the defect but can still be described by a wave vector pointing along the missing row of rods. Such a row a defects acts like a waveguide [20] with a spectrum shown in Fig. 2.

Next, following [3, 4, 6] we introduce two planar-photonic crystal nanocavities (defects) which are spaced aside from the waveguide as shown in Fig. 1b by changing the dielectric constant of defect's material. Each cavity supports a localized single degenerate monopole solution for the TM modes, which has the electric field component parallel to the cylinders [21, 22]. Then each off-channel defect gives rise to the interference of electromagnetic waves flowing over the waveguide and through the off-channel defect, i.e., to the Fano resonance. It results in zero transmission at the defect's eigen frequency ω_0 [4, 23] provided that this frequency belongs to propagation band of the waveguide. Therefore the off-channel defects may serve as perfect mirrors however only at the frequency $\omega = \omega_0$. Then the bound state with the eigen frequency $\omega_c = \omega_0$ might appear between the off-channel defects if the equation

$$r_1(\omega_0) = 1, \quad \theta_m = k(\omega_0)L = \pi m \qquad (2)$$

is fulfilled. It can be done provided that the distance L between defects is quantized. Thus, for the linear systems the phenomenon of formation of the BSC is rather subtle one.

Principally new possibility was found first by Marburger and Felber [24] in the FPR filled by a Kerr-medium, whose refractive index depends on intensity of light as shown in Fig. 1a: $n = n_0 + n_2I$. In the framework of one-dimensional nonlinear Maxwell equations they has shown that the transmission becomes multiple valued as dependent on the incident intensity to give rise respectively to a bistability. This approach was developed in many publications (see in particular, the reference list in [1]). Here we consider a different scheme based on the off-channel defects made from a Kerr medium shown in Figs. 1b, 1c while a medium between defects is linear. We can refer this system as the FPR with nonlinear mirrors. The photonic FPR with nonlinear mirrors also displays the bistability properties. However our main aim is to demonstrate new resonances of very peculiar shape. We argue these are fingerprints of series of the BSCs which become to be coupled with incident wave via the nonlinearity of mirrors of the FPR.
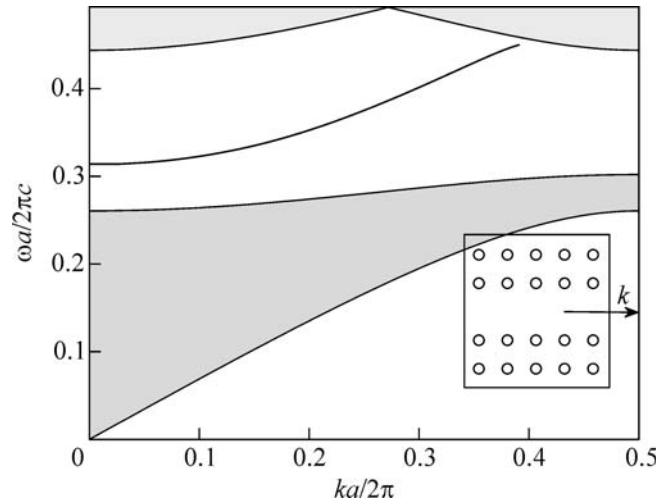
Fig. 2. PC is a square lattice of dielectric rods ($\epsilon = 11.56$) of radius $0.18a$ in air where a is the period. One row of rods is extracted from the PC. The dispersion relation of the propagating guided TM mode is shown by solid line [22].

2. BASIC EQUATIONS

The single nonlinear impurity embedded in a one-dimensional continuum attracted interest long time ago because of analytical treatment and its generality [23, 25–27]. The system is open and differs from closed nonlinear one by that the transmission resonance properties depend on the frequency of incident wave and its amplitude both. The main result is that the transmission coefficient of a single waveguide mode scattering from Kerr off-channel features was shown to exhibit bistability properties arising from the nonlinearity of the off-channel defect. The frequency of isolated bound mode for the single isolated defect cylinder decreases monotonously with growth of its dielectric constant ϵ_d [22, 7]. Therefore the mode frequency of the defects enumerated by $j = 1, 2$ for the radius much less than the EM wave length undergoes shift

$$\omega_j = \omega_0 + \lambda|E_j|^2 \qquad (3)$$

because of the Kerr effect [26]. The transmission through each defect has zero (resonance dip) at these eigen frequencies [23]. In order to the defects were perfect mirrors we are to take the transmission zeros of both defects occur at the same frequency

$$\omega_c = \omega_0 + \lambda X_c = \omega_0 + \lambda Y_c, \qquad (4)$$

where $X = |E_1|^2$, $Y = |E_2|^2$ are intensities of electromagnetic wave at the first and second defects (mirrors) respectively. This equation relates intensities at the defects equaled: $X_c = Y_c$. The condition for the BSCs (2) between nonlinear mirrors give us the next equation for the intensity X_c:

$$k(\omega_0 + \lambda X_c)L \approx k(\omega_0)L + v_g(k_0)\lambda X_c L = \pi m, \quad (5)$$
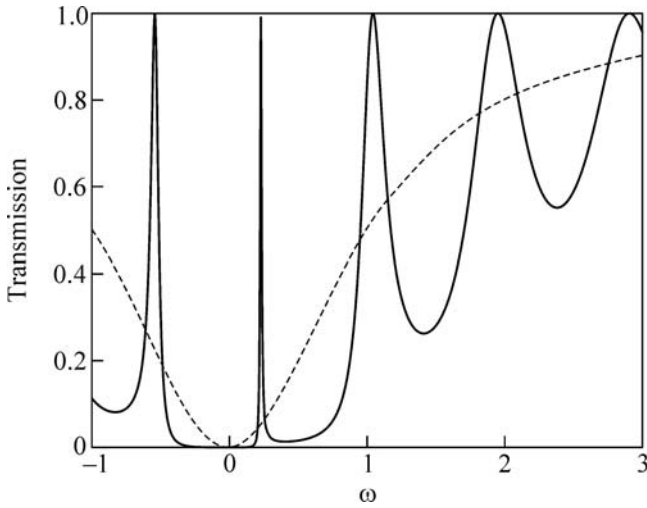
Fig. 3. The transmission in the linear FPR described by the coupled-mode equation (9) for $\omega_0 = 0$, $\Gamma = 1$, $\theta = 0.7\pi + \pi\omega$ (solid line). By dashed line the transmission in the waveguide coupled with the single off-channel defect with the parameters $\omega_0 = 0$, $\Gamma = 1$ is shown.

where k is the wave number of the electromagnetic wave propagated along the waveguide which is function of the frequency ω as shown in Fig. 2. For the linear case $\lambda = 0$ this equation can be fulfilled only by tuning of the distance L between mirrors. However for the nonlinear defects there might be a new possibility to tune the light intensities at the defects.

The transmission of TM modes in linear PC structures is equivalent to quantum transmission [20]. Thereby basic equations for the transmission in the PC structures can be derived from the Lippman–Schwinger equation [3, 4], from the coupled-mode theory [2, 5, 20], or one can explore the tight-binding models [23] with further continual limit $ka \ll 1$. In the present letter we use the second approach of the temporal couple-mode theory. We start with case of single off-channel defect coupled with the single waveguide. Let a monochromatic wave $E_{in}e^{-i\omega t}$ incidents at the left. Then we can write for the defect amplitude

$$\dot{E} = -i\omega_0 E - \frac{2}{\tau}E + \sqrt{\frac{2}{\tau}}E_{in}e^{-i\omega t}. \tag{6}$$

This equation has simple physical meaning. Because of coupling of the defect mode with the waveguide it leaks into there with the decay time τ. Simultaneously owing to the same coupling the source in the form of incident wave in the right hand of Eq. (8) supports the defect mode. For defect with the Kerr nonlinearity (3) we can substitute the time dependence as $E(t) = Ee^{-i\omega t}$ and present Eq. (6) as follows

$$(\omega - \omega_0 + i\Gamma)E = i\sqrt{\Gamma}E_{in}. \tag{7}$$

Further we can write for the transmission amplitude with account of interference of direct path over the waveguide and the path through the off-channel defect

$$t_1 = E_{in} - \sqrt{\frac{2}{\tau}}E. \tag{8}$$

The reflection amplitude equals $r_1 = -\sqrt{2/\tau}\,E$. One can see that for $E = 0$ there is no reflection, and $|r_1|^2 + |t_1|^2 = E_{in}^2$. The transmission for single linear off-channel defect is shown in Fig. 3 by dashed line. The case of single nonlinear off-channel defect was considered on [23]. One can see that the single defect has zero transmission, i.e. perfect reflection at $\omega = \omega_0$.

Now we can easily write the coupled-mode theory equations for the case of two defects separated by distance L with corresponding amplitudes E_1 and E_2 (see, for example, [5]):

$$(\omega - \omega_1 + i\Gamma)E_1 + i\Gamma e^{i\theta}E_2 = i\sqrt{\Gamma}E_{in},$$
$$i\Gamma e^{i\theta}E_1 + (\omega - \omega_2 + i\Gamma)E_2 = i\sqrt{\Gamma}e^{i\theta}E_{in}, \tag{9}$$

and the transmission amplitude

$$t = E_{in}e^{i\theta} - \sqrt{\Gamma}E_1 e^{i\theta} - \sqrt{\Gamma}E_2, \tag{10}$$

where $\theta = k(\omega)L$ represents the phase shift incurred as the waveguide mode travels from the first defect to the second one. From (9) we obtain

$$E_1 = \frac{i\sqrt{P}[\tilde{\omega} + \epsilon + i\Gamma(1 - e^{2i\theta})]}{\tilde{\omega}^2 - \epsilon^2 + 2i\Gamma\tilde{\omega} - \Gamma^2(1 - e^{2i\theta})},$$
$$E_2 = \frac{i\sqrt{P}e^{i\theta}(\tilde{\omega} - \epsilon)}{\tilde{\omega}^2 - \epsilon^2 + 2i\Gamma\tilde{\omega} - \Gamma^2(1 - e^{2i\theta})}, \tag{11}$$

where

$$\tilde{\omega} = \omega - \frac{\omega_1 + \omega_2}{2} = \omega - \omega_0 + \frac{\lambda}{2}(X + Y),$$
$$\epsilon = \frac{\omega_1 - \omega_2}{2} = \frac{\lambda}{2}(X - Y), \tag{12}$$

the value $P = \Gamma|E_{in}|^2$ is proportional to the input wave power. Substituting (11) into (12) we obtain the non-linear self-consistent equations for EM intensities X and Y at each defect

$$X[(\tilde{\omega}^2 - \epsilon^2 - 2\Gamma^2\sin^2\theta)^2 + \Gamma^2(2\tilde{\omega} + \Gamma\sin 2\theta)^2]$$
$$= P[(\tilde{\omega} + \epsilon + \Gamma\sin 2\theta)^2 + \Gamma^2\sin^4\theta],$$
$$Y[(\tilde{\omega}^2 - \epsilon^2 - 2\Gamma^2\sin^2\theta)^2 + \Gamma^2(2\tilde{\omega} - \sin 2\theta)^2]$$
$$= P(\tilde{\omega} - \epsilon)^2, \tag{13}$$

which is the system of nonlinear algebraic self-consistent equations via Eqs. (12).

3. RESONANCES AT BOUND STATES IN CONTINUUM

The solution of Eq. (9) is given by the inverse of the left matrix in (9). However there might be the special case when the inverse does not exist for the determinant of the matrix equaled to zero

$$\tilde{\omega}^2 - \epsilon^2 - 2\Gamma^2 \sin^2\theta = 0,$$
$$\tilde{\omega} = -\Gamma \sin\theta \cos\theta$$

at the points

$$\epsilon = 0, \quad \tilde{\omega} = 0, \quad \theta_m = \pi m. \tag{14}$$

After substitution notations (12) and $\theta = kL$ one can see easily that Eq. (14) is equivalent to Eqs. (4), (5). At the point (14) the solution of Eq. (9) is $E_1 + E_2 e^{i\theta_m} = 0$ and exists for zero incident wave $E_{in} = 0$. Therefore the homogeneous solution is localized at the defects and corresponds to the BSC [28, 15].

The dispersion relation shown of the propagating guided mode shown in Fig. 2 for photonic crystal waveguide has complicated form and can be calculated only numerically [22]. However near the resonance frequencies of the defects one can use the linear approximation and write for the phase shift

$$\theta(\omega) = \theta_0 + \theta_1\omega. \tag{15}$$

The intensities of BSCs at the defects are coincided $X_c = Y_c$. Then Eq. (4) gives us $X_c = (\omega_c - \omega_0)/\lambda$. Substituting (15) and this equality into (5) we obtain

$$X_{cm} = \frac{\pi m - \theta_0}{\lambda\theta_1}. \tag{16}$$

Thus the FPR with nonlinear mirrors can capture electromagnetic wave irrespective to the distance between mirrors if the intensity of the wave is quantized at the defects. The transmission and the intensities were computed numerically for small incident amplitude $E_{in} = 0.1$ and presented in Figs. 4 and 5, respectively. A part of the transmission which is very close to the linear case (Fig. 3) is shown by dashed line in Fig. 4a. However a nonlinearity of the defects gives rise to a new series of a picket-fence like resonances, and each resonance has rather complicated shape as shown in Fig. 4b. To be specific we took $\lambda = 0.2$, $\omega_0 = 0$, $\theta_0 = 0.7\pi$, $\theta_1 = \pi$. If to substitute these values into Eq. (16) we obtain that the BSC frequencies equal $0.3 + n = 0.3, 1.3, 2.3, ...$ and the intensities do $5(0.3 + m) = 1.5, 6.5, 11.5, ...$ One can see that these values exactly agree with the positions of new resonances in Fig. 4 and corresponding intensities shown in Fig. 5.

The definition of the BSCs as localized (square integrable) ones is equivalent to that they have zero resonance width [15]. The resonance positions and resonance widths are given the complex eigen values of
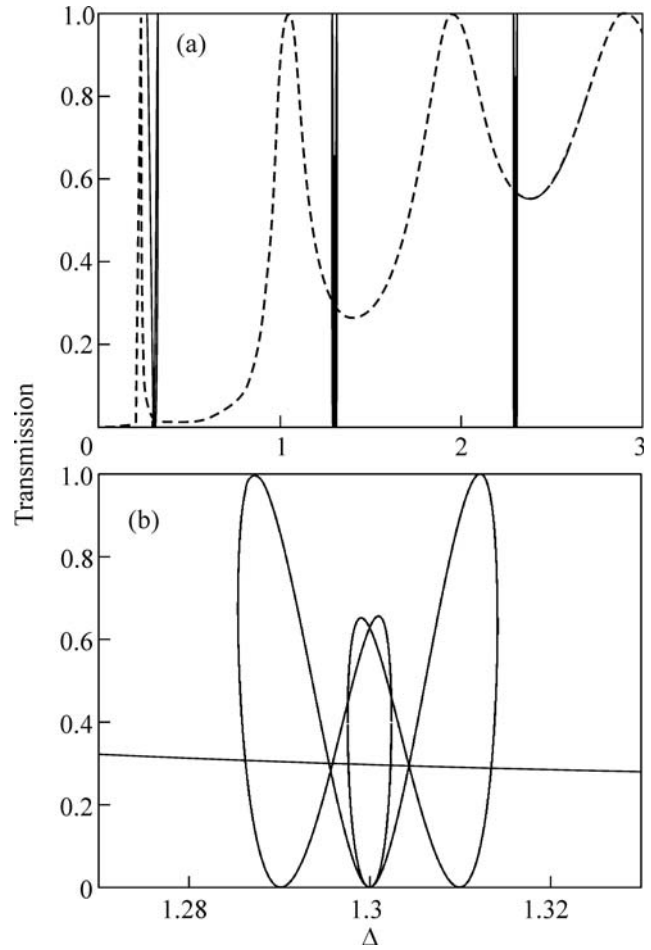
Fig. 4. (a) Transmission spectra as dependent on frequency in the FPR given by Eq. (9) for the nonlinear case $\lambda = 0.2$. The parameters of the FPR are $\omega_0 = 0$, $\Gamma = 1$, $\theta = 0.7\pi + \pi\omega$, $E_{in} = 0.1$. Dash line shows those part of the transmission which is close to that for the linear FPR shown in Fig. 3 for small E_{in}, solid line does the transmission features induced by BSCs (BSC resonances). (b) Blowup of the BSC resonance for the BSC frequency equaled to 1.3.

the effective Hamiltonian [29] which is the left hand matrix in (9):

$$z_{1,2} = \frac{\omega_1 + \omega_2}{2} - i\Gamma \pm \sqrt{\epsilon^2 - \Gamma^2 \exp(2i\theta)}. \tag{17}$$

From where we obtain that at the point (14) one resonance becomes infinitely narrow ($\text{Im}(z_1) = 0$) while the second one acquires the maximal width 2Γ [3, 5, 6]. The last resonance behavior is illustrated in Fig. 6. Therefore the point (14) is the BSC, indeed. At this point there is the homogeneous solution of the coupled mode Eq. (9)$|\text{BSC}\rangle = \begin{pmatrix} 1 \\ -e^{i\theta_m} \end{pmatrix} = \begin{pmatrix} 1 \\ \mp 1 \end{pmatrix}.$

This solution is localized at the impurity states. As known from linear algebra [30] the necessary and sufficient condition for the existence of the inhomoge-
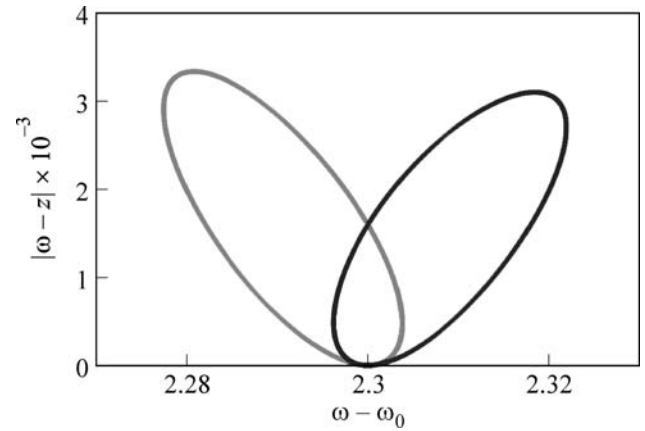
Fig. 6. Color online. The frequency behavior of complex eigen values $|z_{1,2} - \omega|$ (17) zero of which gives the BSC in the nonlinear FPR.

Fig. 5. (a) The general solution of Eq. (13) for the parameters given in Fig. 4. (b) Color online. Blow up of solutions near the BSC frequency $\omega_c = 1.3$: X (blue line) and Y (red line).

neous solution of Eq. (9) for $\phi_{in} \neq 0$ is that the left vector $(BSC| = (1 - e^{i\theta_m}) = (1 \mp 1)$ is to be orthogonal to the incoming vector $(1\, e^{i\theta_m}) = (1 \pm 1)$. It holds indeed for the linear case. Then the general solution of Eq. (9) at the BSC point can be given [16]

$$|\psi\rangle = \alpha|BSC\rangle + E_{in}\begin{pmatrix} 1 \\ e^{i\theta_m} \end{pmatrix}, \qquad (18)$$

where α is an arbitrary coefficient and the second term is the particular transport solution of Eq. (9). The orthogonality of the BSC to incoming wave vector implies that the BSC state is not coupled to the continuum and therefore there can not be a resonance at its discrete frequency ω_c given by (4).

However that is *not the case* for the nonlinear FPR. The nonlinearity violates the linear superposition (18). As the result a coupling between the BSC and incoming wave appears because of nonlinearity. Therefore

the incoming wave excites the BSC. Moreover the BSC exists in a whole range of the length L between the nonlinear mirrors. Numerics indeed shows completely new type of resonances for the nonlinear FBR as shown in Fig. 2. One can see that the positions of these resonances are in full agreement with formulas (5).

In conclusion let us compare the FPR with nonlinear media between linear mirrors considered by Marburger and Felber and the present FPR with nonlinear off-channel defects. In both types of the nonlinear FPRs the transmission is multiple valued as the function of the frequency or incident intensity. However the former FPR supports bound state in continuum only if the mirror is perfect, i.e. the reflectance equals unit. In that view the FPR filled my nonlinear media is similar to the linear FPRs [2–7]. In the FPR considered in the present letter the nonlinear off-channel defects self induce the transmission zeroes at whole discrete sequence of the light intensity to give rise to a corresponding sequence of bound states between the off-channel nonlinear defects. Moreover these solutions exist for $E_{in} = 0$, that determines them as the bound states in continuum (BSC). On the other hand, the nonlinearity of the off-channel defects provides a coupling of incident wave with the BSCs to cause new resonances at their eigen frequencies. Moreover as seen in Fig. 4 the FPR might be transparent in the vicinity of these resonances. In conclusion we note that the results presented here can be considered as a special case of the two-level nonlinear Fano–Anderson model [31].

REFERENCES

1. R. Reinisch, G. Vitrant, and H. Haelterman, Phys. Rev. B **44**, 7870 (1991).
2. C. Manolatou, M. J. Khan, S. Fan, et al., IEEE J. Quantum Electron. **35**, 1322 (1999).
3. S. Fan, P. R. Villeneuve, J. D. Joannopoulos, et al., Phys. Rev. B **59**, 15882 (1999).
4. Y. Xu, Y. Li, R. K. Lee, and A. Yariv, Phys. Rev. B **62**, 7389 (2000).
5. Z. Wang and S. Fan, Phys. Rev. E **68**, 066616 (2003).
6. L.-L. Lin, Z.-Y. Li, and B. Lin, Phys. Rev. B **72**, 165330 (2005).
7. E. N. Bulgakov and A. F. Sadreev, Phys. Rev. B **78**, 075105 (2008).
8. C. S. Kim and A. M. Satanin, Phys. Rev. B **58**, 15389 (1998).
9. I. Rotter and A. F. Sadreev, Phys. Rev. E **69**, 066201 (2004); Phys. Rev. E **71**, 046204 (2005).
10. A. F. Sadreev, E. N. Bulgakov, and I. Rotter, Phys. A: Math. Gen. **38**, 10647 (2005).
11. G. Ordonez, K. Na, and S. Kim, Phys. Rev. A **73**, 022113 (2006).
12. J. von Neumann and E. Wigner, Phys. Z. **30**, 465 (1929).
13. F. H. Stillinger and D. R. Herrick, Phys. Rev. A **11**, 446 (1975).
14. C. Texier and G. Montambaux, J. Phys. A **34**, 10307 (2001).
15. E. N. Bulgakov, I. Rotter, and A. F. Sadreev, Phys. Rev. A **75**, 067401 (2007).
16. E. N. Bulgakov, K. N. Pichugin, A. F. Sadreev, and I. Rotter, JETP Lett. **82**, 498 (2005).
17. A. Z. Devdariani, V. N. Ostrovsky, and Yu. N. Sebyakin, Sov. Phys. JETP **44**, 477 (1976).
18. H. Friedrich and D. Wintgen, Phys. Rev. A **32**, 3231 (1985).
19. F. Capasso et al., Nature (London) **358**, 565 (1992).
20. J. Joannopoulos, S. G. Johnson, J. N. Winn, and R. D. Meade, *Photonic Crystals: Molding the Flow of Light* (Princeton Univ., Princeton, NJ, 2008).
21. P. R. Villeneuve, S. Fan, and J. D. Joannopoulos, Phys. Rev. B **54**, 7837 (1996).
22. K. Busch, S. F. Mingaleev, A. Garcia-Martin, et al., J. Phys.: Cond. Mat. **15**, R1233 (2003).
23. A. E. Miroshnichenko, S. F. Mingaleev, S. Flach, and Yu. S. Kivshar, Phys. Rev. E **71**, 036626 (2005).
24. J. H. Marburger and F. S. Felber, Phys. Rev. A **17**, 335 (1978).
25. M. I. Molina and G. P. Tsironis, Phys. Rev. B **47**, 15330 (1993).
26. A. R. McGurn, Chaos **13**, 754 (2003); J. Phys.: Cond. Mat. **16**, S5243 (2004).
27. S. Longhi, Phys. Rev. B **75**, 184306 (2007).
28. M. Miyamoto, Phys. Rev. A **72**, 063405 (2005).
29. I. Rotter, Rep. Prog. Phys. **54**, 635 (1991).
30. V. I. Smirnov, *A Course of Higher Mathematics* (Pergamon, Oxford, 1964), Vol. 3, Part 1.
31. E. N. Bulgakov and A. F. Sadreev, Phys. Rev. B **80**, 115308 (2009).